

Author's Accepted Manuscript

SHINE: Web application for determining the Horizontal stress orientation

Michele M.C. Carafa, Gabriele Tarabusi, Vanja Kastelic



PII: S0098-3004(14)00224-6
DOI: <http://dx.doi.org/10.1016/j.cageo.2014.10.001>
Reference: CAGEO3443

To appear in: *Computers and Geosciences*

Received date: 19 March 2014
Revised date: 23 September 2014
Accepted date: 1 October 2014

Cite this article as: Michele M.C. Carafa, Gabriele Tarabusi and Vanja Kastelic, SHINE: Web application for determining the Horizontal stress orientation, *Computers and Geosciences*, <http://dx.doi.org/10.1016/j.cageo.2014.10.001>

This is a PDF file of an unedited manuscript that has been accepted for publication. As a service to our customers we are providing this early version of the manuscript. The manuscript will undergo copyediting, typesetting, and review of the resulting galley proof before it is published in its final citable form. Please note that during the production process errors may be discovered which could affect the content, and all legal disclaimers that apply to the journal pertain.

1 SHINE: Web Application for Determining the Horizontal Stress
2 Orientation

3
4 Michele M. C. Carafa¹, Gabriele Tarabusi^{2,3}, Vanja Kastelic¹

5
6
7
8 ¹Istituto Nazionale di Geofisica e Vulcanologia - INGV, Via dell'Arcivescovado 8, L'Aquila,
9 Italy

10
11 ²Istituto Nazionale di Geofisica e Vulcanologia – INGV, Via di Vigna Murata 605, Roma, Italy

12
13 ³Università degli Studi di Ferrara, Dipartimento di Fisica e Scienze della Terra, Via Saragat 1,
14 Ferrara, Italy

15
16 Corresponding Author:
17 Michele M.C. Carafa
18 Email: michele.carafa@ingv.it;

19
20

21 **ABSTRACT**

22 Interpolating the orientation of the maximum horizontal compressive stress with a well-
23 established procedure is fundamental in understanding the present-day stress field. This
24 paper documents the design principles, strategies and architecture of SHINE
25 (<http://shine.rm.ingv.it/>), a web-based application for determining the maximum
26 horizontal compressive stress orientation. The interpolation using SHINE can be carried
27 out from a global database or from a custom file uploaded by the user. SHINE satisfies
28 the usability requirements by striving for effectiveness, efficiency and satisfaction as
29 defined by the International Organization for Standardization (ISO) covering
30 ergonomics of human-computer interactions. Our main goal was to build a web-based
31 application with a strong “outside-in” strategy in order to make the interpolation
32 technique available to a wide range of Earth Science disciplines. SHINE is an easy-to-
33 use web application with a straightforward interface guaranteeing quick visualization of
34 the results, which are downloadable in several formats. SHINE is offered as an easy and
35 convenient web service encouraging global data sharing and scientific research

36 collaboration. Within this paper, we present a possible use of SHINE, determining fault
37 kinematics compatibility with respect to the present-day stress field.

38

39 Keywords: Present-day stress, web application, maximum horizontal compressive stress, horizontal stress
40 interpolation, stress maps.

41 **1. Introduction**

42

43 An important measure of the deformation state within the Earth's crust is the orientation
44 of the maximum horizontal compressive stress (SHmax), which is determined from
45 different types of geophysical data, such as earthquake focal mechanisms, well bore
46 breakouts, and fault-slip analysis. Several local, regional or world-wide SHmax
47 databases are available; the most complete and detailed compilation of the
48 contemporary crustal stress field is the World Stress Map Release 2008 (WSM08;
49 Heidbach et al., 2008). The WSM08 database contains 21,750 quality-ranked stress data
50 records using a constantly updated and refined scheme based on different measurement
51 aspects, such as the accuracy or the depth (Zoback and Zoback, 1989; Sperner et al.,
52 2003). Each stress data record has a quality factor assigned, ranging from A (the
53 highest; standard deviations of data records within $\pm 15^\circ$) to E (the lowest; standard
54 deviations greater than $\pm 40^\circ$). This quality ranking scheme is usually used as a reference
55 standard for local compilations and stress indicators comparisons on a global scale.

56 Despite the large number of SHmax data sources, none of the available databases can
57 estimate the state of stress for points not corresponding to the exact location of the
58 SHmax data record. To obtain SHmax orientation for any point on the Earth's surface, it
59 is necessary to perform an interpolation or smoothing procedure. Several such methods
60 (Lee and Angelier 1994, Coblenz and Richardson 1995, Bird and Li, 1996; Mueller et
61 al. 2003; Carafa and Barba 2013) have been proposed, but none of them have been

62 implemented into a freely available web application. The scope of this paper is the
 63 description of SHINE (SH INtErpolation) web application, that calculates the SHmax
 64 orientation for any chosen point worldwide.

65 **2. Theory**

66

67 SHINE implements the Carafa and Barba (2013) interpolating method. We present the
 68 main aspects of this interpolation scheme, which modified and extended the clustered
 69 data analysis technique used by Bird & Li (1996). We refer the readers to the Carafa
 70 and Barba (2013) study for an extensive explanation of the method, while we only point
 71 out its main aspects.

72

73 Let x be a point where we wish to estimate the stress orientation, and let us select only
 74 the data points within a θ range (angular distance or searching radius), varying from 0°
 75 to 180° . Carafa and Barba (2013) conducted an extensive study to determine the
 76 probability of finding an azimuth at x , given one datum r located at range θ . The
 77 probability P^* can be expressed as:

78

$$P^*(k(\alpha_r)|\alpha_s) \equiv P^*(k_r|s) = P_0^* + P_1^* \exp(-\theta/\theta_0), \quad (1)$$

79

80 where θ_0 , P_0^* and P_1^* are constants determined from a nonlinear least-squares fit of the
 81 empirical probabilities determined on the global scale by Carafa and Barba (2013) using
 82 the WSM08 dataset.

83

84 After data selection, it is important to decluster the input data to avoid overweighting
 85 the local sources of stress characterized by numerous measurements (and data record

86 entries) close together. In the method proposed by Bird and Li (1996) and Carafa and
 87 Barba (2013), a pair of stress data points r and s form a cluster if:

88

$$P^*(s|r) > \max_{i=r,s} P^*(i|x), \quad (2)$$

89

90 i.e. the conditional probability of r and s is larger than the highest possible conditional
 91 probability with respect to the interpolation point x . The opposite defines the two data
 92 records as independent clusters. In equation 2, we simplify the notation by using the
 93 indices r and s in place of azimuths α_r and α_s . We adopt such notation for the
 94 following equations. After clusters have been defined, a two-pass procedure is applied
 95 to find the SHmax orientation at x . In the first step, the clustered data are pre-averaged,
 96 resulting in a set of fully independent SHmax orientations. In the second step, the
 97 SHmax orientation is interpolated on x . The pre-averaged values of the clustered data
 98 are obtained in the first step using two-point conditional probability distributions,
 99 assuming no azimuthal dependence between the data. The SHmax orientation of the
 100 cluster is assigned to its geographical centre.

101

102 In the next step, the SHmax orientations are interpolated on x . To identify the now fully
 103 independent orientations, identified as “clusters” and labelled as c regardless of whether
 104 they arose from pre-averaging, we calculate the probability for each trial azimuth,
 105 defined by an integer value of k_x ($k_x = 1, \dots, 60$ with 3° bins), as:

$$P_{N_c}^*(\mathbf{k}_x) = \frac{\prod_{c=1}^{N_c} P^*(k_x|c)}{\sum_{j=1}^{60} \prod_{c=1}^{N_c} P^*(j_x|c)}, \quad (3)$$

106 where N_c is the number of clusters within the θ_n range (Eq. 2). The maximum
 107 likelihood estimate of the SHmax orientation at the interpolation point x is:

$$\alpha_x = \left(k_x - \frac{1}{2}\right) 3^\circ, \quad (4)$$

108 where k_x is the integer that maximises $P_{N_c}^*(k_x)$ in Eq. (10). The 90% confidence
 109 interval $\Delta\alpha$ is determined as:

110

$$\int_{\alpha_x - \Delta\alpha}^{\alpha_x + \Delta\alpha} p_N^*(\alpha'_x \bmod 180^\circ) d\alpha'_x = 0.90, \quad (5)$$

111 where $p_N^*(\alpha'_x \bmod 180^\circ)$ is the functional form corresponding to the discrete $P_N^*(k_x)$ and
 112 “mod” is the remainder of the integer division used to account for the periodicity of α'_x .

113 This procedure allows the uncertainties due to data scattering to propagate into the
 114 posterior uncertainties $\Delta\alpha$.

115

116 A well-defined SHmax orientation, especially at the local scale, is ensured by three
 117 factors: 1) a relative high cluster number N_c , 2) a narrow 90% confidence interval $\Delta\alpha$
 118 and 3) a small relative range (or searching radius). These three are the most important
 119 factors in obtaining a SHmax orientation for any chosen point on the Earth's surface.
 120 Therefore, they need to be entered in the SHINE engine and carefully set by the user.

121 **3. WEB site design principles, strategies and architecture**

122

123 **3.1. Designing principles for SHINE website**

124

125 The main goal of SHINE website (<http://shine.rm.ingv.it/>) is to determine SHmax at any
 126 chosen interpolation point worldwide using the approach of Carafa and Barba (2013)
 127 (Figure 1). A distinct advantage of SHINE is the integration of significant amount of
 128 information and theory in a single package which provides all users with an advanced
 129 analysis tool regardless of their individual theoretical background. We follow the
 130 guidelines prescribed by Part 11 of the ISO 9241 standard (BSI, 1998) to define SHINE

131 usability as “the extent to which a product can be used by specified users to achieve
132 specified goals with effectiveness, efficiency and satisfaction in a specified context of
133 use.”

134 For this application we defined:

- 135 – Effectiveness as the ability of researchers to obtain SHmax results from SHINE;
- 136 – Efficiency as a minimum amount of time consumed by researchers using SHINE
137 in relation to the accuracy and completeness of SHmax results;
- 138 – Satisfaction as the "ease in operation" for researchers to apply SHINE as a
139 useful research tool.

140

141 Our primary goal for SHINE was to optimize its usability by researchers who have the
142 need for effective and efficient means to evaluate the intraplate stress field. In order to
143 address this aim we contacted seven geosciences researchers as a representative sample
144 of SHINE website users and involved them in the prototype development. They tested
145 several versions of the web interface and provided valuable feedback. Consequently we
146 made the website design and development process iterative to optimize the researchers’
147 feedback.

148

149 During SHINE development, we followed the suggestions of Stone et al. (2010) for the
150 main aspects of web design. The design principles for SHINE are based around the
151 HOME RUN idea, which stands for High quality content, Often updated, Minimal
152 download time, Ease of use, Relevant to user’s needs, Unique to the online medium,
153 and Net-centric corporate culture (Nielsen, 2000). A HOME RUN is, in other words, a
154 criterion that SHINE had to pass at every stage to meet the users’ requirements. Two
155 SHINE examples of applying HOME RUN principles are: 1) web pages were designed
156 to be read quickly and easily with a short loading time that was obtained by using no
157 more graphics than necessary; and 2) SHINE works with any web browser.

158

159 **3.2. Design strategies**

160

161 During SHINE prototyping, the test-users/researchers needed to carefully analyze the
162 interpolation scheme of Carafa and Barba (2013) and asked for detailed explanations on
163 SHINE functionality. For this reason we adopted the strategy of building SHINE start
164 page (Figure 2). We used it to meet the users' expectation for sufficient explanation of
165 SHINE's basic characteristics. Moreover, the start page provides an opportunity to
166 suggest additional stress tensor information, literature and web pages.

167

168 The core of SHINE website is the form on the input page, which opens once the user
169 starts the session. We carefully considered design strategies for this part of the
170 application because it is the user's main interaction with SHINE. We decided to create
171 the interaction with an "outside-in" strategy, thus building SHINE from the perspective
172 of a researcher not used to frequently interpolate data. Consequently, our strategic
173 choice was a form composed of several sections in one long web page. To further help
174 the users, each section and sub-section of the web form has an on-line help on a semi-
175 transparent java script overlay, which can be opened, closed or moved within the web
176 page and guides the user throughout the selection procedure.

177

178 In the web form, we used drop down lists and sliders with fixed step values and a
179 geographical interface for selecting and displaying the input. We believe that this
180 strategy guides the user and minimizes the possibility of error in choosing the input
181 parameters. At the same time, the possibility of uploading custom SHmax data and
182 selecting scattered points to perform the calculation allows for a high level of input data
183 customization.

184

185 All the labels of the form are right or top-aligned. Wroblewki (2010) explained that
186 forms with this mixed alignment of labels take longer to complete because they require
187 a number of eye fixations to parse. We intentionally decided to use label mixing,
188 because we strive for slower completion to increase the awareness of researchers filling
189 in the form. In fact, during the prototyping phase, we observed that higher completion
190 time obliged researchers to slow down and carefully consider each help text associated
191 with each field of the form. For the help text, we needed to choose between dynamic
192 help systems that can be automatically triggered/accessed by the user or always visible
193 help text. Because we ask for complex inputs, we always chose the visible help text so
194 users can benefit from it in every step.

195

196 To assure correctness of all the input parameters and to avoid duplicate entries
197 throughout the input selection, we repeatedly used text messages that served as
198 acceptance confirmation of the selected input parameters. After filling in the input
199 parameters and confirming the form, the actual interpolation process takes place on the
200 host server. A dense interpolation point grid selection implies considerable calculation
201 time and a long wait time for the results. Nah (2004) showed that after 50 seconds of
202 waiting, 90% of web users leave a webpage despite the presence of a feedback bar.
203 Considering this observation, the user's awareness of SHINE's calculation complexity
204 and feedback messages appearing before the results visualization, we set SHINE user
205 tolerable wait time to 50 seconds. Currently (September 2014), the server hosting
206 SHINE calculates 1000 SHmax orientations in 50 seconds; consequently, we forced the
207 upper limit of the number of interpolation points to be 1000. In the future, we expect to
208 raise this limit based on the computational performance of the SHINE hosting server
209 and its related software. Because the calculation step takes time to complete and this

210 fact has to be appropriately communicated to increase the user's wait time tolerance, we
211 inserted a feedback bar that indicates the progress of calculations.
212 Our decision was to present the SHmax output through a graphical interface and to
213 furnish a link for downloading the SHINE results as a zipped folder containing several
214 GIS-supported formats.

215

216 **3.3. Server Platform and programming languages**

217 Currently SHINE website is developed in HTML and hosted on a 64-bit
218 computer/server with PHP (vers. 5.1 or above), GNUWIN
219 (<http://gnuwin32.sourceforge.net>), FWTools (<http://fwtools.maptools.org/>) and HTTP
220 services. The server-side procedures are developed in the PHP language, the client-side
221 in JavaScript language, using specific features of the jQuery (<http://jquery.com/>) and
222 Dojo (<http://dojotoolkit.org/>) libraries and Google Maps API
223 (<https://developers.google.com/maps/>) to provide a geographic interface. The actual
224 calculation part of the application starts on the hosting server through the PHP. Two
225 executables, developed with the Autoit software (<http://www.autoitscript.com>), analyze
226 the uploaded TXT files and create geographic files in Mapinfo Professional MID/MIF
227 format and the KML language (<https://developers.google.com/kml/documentation/>),
228 which is an XML notation for expressing geographic annotation and visualization
229 within Internet-based, two-dimensional maps and three-dimensional Earth browsers. A
230 command line procedure uses FWTools to convert the MID/MIF files into Esri
231 Shapefile format.

232

233

234 **4. HOW TO: SHINE functionality**

235

236 SHINE can be accessed at <http://shine.rm.ingv.it/>. After reading the basic description
237 and functions of SHINE interpolation on the start page, the user can start his/her own
238 session by pressing the “START SESSION” button. The user is redirected to the input
239 page, which consists of the input form divided into three sections: "Data selection",
240 "Geographical setting" and "Strategic parameters".

241

242 When opening the input page, three objects are displayed (Figure 2):

- 243 1) the “Data selection” section;
- 244 2) an interactive map based on Google Maps; and
- 245 3) a grey box at the top of the page, which, in real time, shows the choices made by
246 the user during the form compilation. The "Restart" button on the right side of
247 the grey box allows the user, at any time, to return to the home page, resetting
248 the whole work session.

249

250 The interactive map is centred on L’Aquila city (central Italy). This is the authors'
251 choice because they are currently paid by a project that started after the 2009 L’Aquila
252 earthquake and studies Central Apennines neotectonics and seismic hazard. The
253 interactive map allows the user to move anywhere across the world with the "PAN"
254 command, as provided by GoogleMaps.

255 **4.1. “Data selection”: editing and loading SHmax input dataset**

256 In the “Data selection” section, the user decides which dataset to use when performing
257 the SHmax interpolation (Figure 3). By choosing "WSM08", the user decides to use the
258 World Stress Map, release 2008 (Heidbach et al. 2008) (only A-, B- and C- quality data

259 records); by choosing "FILE", the user decides to upload his/her own file (max 40000
260 data entries allowed) containing the SHmax orientation input dataset. After uploading
261 their own file, the button "check file" performs a series of checks on the size, row
262 number and file structure to ensure that the input file corresponds to the specifications
263 required by the interpolation scheme. If all the requirements are present in the input file,
264 the "PLOT" button appears. After pressing the "PLOT" button, SHINE plots the chosen
265 dataset (WSM08 or custom file) on the interactive map, and the user gets to inspect the
266 chosen input.

267

268 **4.2. "Geographical setting": choosing the study area**

269 In the "Geographical setting" section, the user gets to decide whether to perform the
270 interpolation calculation on a regular grid of points ("Regular area selection") or on a
271 custom user-imported point file ("Custom input file").

272

273 By choosing "Regular area selection" (Figure 4), the user needs to set the limits of the
274 study area by filling the "Longitude" and "Latitude" fields manually in a $-180/180^\circ$ and
275 $-90/90^\circ$ convention, respectively, or by dragging and resizing the red rectangle
276 displayed on the interactive map. After the area bounds definition, the user selects the
277 desired grid spacing from the proposed values in the drop-down list. If the grid spacing
278 selection has been performed appropriately, the "Check grid density" button is enabled.

279 If the number of nodes is less than or equal to the upper limit, (currently set to 1000),
280 the "PLOT" button is enabled, otherwise the user has to lower the grid resolution or to
281 reduce the dimensions of the investigation area to be within the current maximum of
282 1000 interpolation points.

283

284 By choosing "Custom input file", the user decides to perform the interpolation on a
285 custom set of geographical points saved in a properly structured input file. The proper
286 structure is shown in an example file linked to the Custom input file" selection. The
287 button "check file" starts a security check procedure before uploading the user file to the
288 server. At this stage, if all checks are passed, the "PLOT" button is enabled, otherwise it
289 is necessary to follow the warning indications displayed on the screen.

290

291 The final step for both the "Regular area selection" or the "Custom input file" choice is
292 the visualization of the chosen interpolation points. This step occurs when the user
293 presses the "PLOT" button and chosen interpolation points are displayed as red crosses
294 on the geographical map.

295 **4.3. "Strategic Parameters": deciding the interpolation scheme**

296 In this section (Figure 5), the user needs to properly set the three main parameters of the
297 interpolation scheme of Carafa and Barba (2013) (see Section 2):

- 298 – "Searching radius": by moving the slider, the user sets the data-points maximum
299 distance from the interpolation point. Data points not exceeding the user-
300 determined distance are used in the interpolation scheme. Because the method of
301 Carafa and Barba (2013) determines the probabilities on concentric annuli, the
302 slider is set to fixed distances (corresponding to the external limit of the selected
303 annulus). A suggested annulus value for local scale interpolation is two or three
304 (corresponding to 58-96 km); a suggested annulus value for interpolation on a
305 wider scale is six to eight (228-327 km).
- 306 – "Minimum cluster" slider: it sets the minimum number of clusters (not data)
307 surrounding the interpolation point to accept the SHmax result as "stable".
308 Suggested value is three.

309 – "90% confidence limits": by moving the slider, the user decides the maximum
310 permissible uncertainty. Any SHmax input value with confidence level greater
311 than the one set, is not considered stable or representative. A suggested value is
312 between 30° and 50°.

313

314 After completing the "Strategic parameters" section, the user needs to click the "I agree
315 and move forward" button to proceed with the calculation. A dialog box appears
316 displaying all of the choices made by the user so far. At this step, two options are
317 available:

- 318 – "Cancel": SHINE redirects the user to the "Strategic parameters" section;
- 319 – "OK": the user confirms all previous choices and the calculation procedure
320 starts. After selecting the "OK" option, in a few seconds (depending on the
321 number of interpolation points and the average data records falling inside the
322 searching radius of each interpolation point) the results page opens and the stress
323 map is presented.

324

325 **4.4. Stress map visualization**

326

327 On the results page, four main elements are displayed (Figure 6):

- 328 – a grey box at the top of the page displaying the choices made by the user in the
329 input form;
- 330 – a Google Maps based graphical interface displays two distinct levels: the SHmax
331 input dataset chosen by the user (black colored lines), while the interpolation
332 calculation results (output layer) are presented in red for the maximum
333 horizontal stress orientation values calculated for the points selected by the user.

334 By clicking on the tooltip (balloon) located at each interpolation point in the
335 output layer, the user can read the geographic coordinates, SHmax orientation
336 (in degrees) and related quantities (90% confidence level bounds, searching
337 radius, cluster number and used stress-data records).

338 – "Download results in zip format" link allows the user to download results in
339 different formats (including several spatial data formats supported by GIS
340 software).

341 – - The “click here for a new interpolation/stress map” button redirects the user to
342 the SHINE starting page.

343 ***5. Application of SHINE in testing active fault's slip compatibility*** 344 ***within the present-day stress regime***

345
346 In the study of active faults, an important parameter to consider is the compatibility of
347 the recognized fault with respect to the present-day stress field. Geological methods,
348 paired with geomorphic studies, provide data for the fault's existence, but may not be
349 sufficient in evaluating its activity. In cases of lack of seismicity and where rocks or
350 sediments do not provide a record of recent fault-related deformation, the interpolated
351 local-stress orientation can provide important constrain for possible recent slip activity
352 along the fault. SHINE provides a valuable tool for the calculation of the SHmax
353 orientation along active faults. Notably, to avoid the potential for circular reasoning, the
354 dataset used in the fault parameterization (e.g., fault-slip analysis or earthquake focal
355 mechanisms) should not be the same dataset as the one used in SHINE to interpolate
356 SHmax orientations.

357 We choose Slovenia as a case study to examine and compare the observational data on
358 active faults with the SHINE-derived local stress field. The country is an amalgam of

359 several structure units (i.e. Southern Alps, External Dinarides, and Panonian Basin).
360 The predominant geometry of the active faults is NW-SE oriented trend, towards NE
361 dipping and dextral strike-slip kinematics (Placer, 1998; Poljak, 2000; Kastelic et al.,
362 2008; Kastelic and Carafa, 2012; Basili et al., 2013). This trend is particularly strong in
363 the western and central part of the country, while the eastern sectors show the
364 prevalence of the Mid-Hungarian tectonic imprint, with a NE-SE trend (Vrabec and
365 Fodor, 2006). Slovenia has been seismically active during historic and instrument
366 observation periods with frequent $M > 5$ earthquakes (Živčić, 2010; Stucchi et al., 2013).
367 To carry out SHINE analysis on fault compatibility, we utilized the European database
368 on the European database of seismogenic faults - EDSF (Basili et al., 2013). From this
369 database we extracted the seismogenic faults in Slovenia and its close vicinity. In total,
370 we considered 42 seismogenic faults and their corresponding 258 interpolation points
371 (representing sections of faults with slight changes in their geometrical parameters) that
372 were fully parameterized in their geometric and kinematic characteristics. We assumed
373 that the strike, dip and rake assigned to each interpolation point are defined by a
374 uniform probability distribution in the minimum - maximum interval of the
375 corresponding EDSF's fault characteristics.

376

377 We employed a forward analysis of the fault orientation data to evaluate the optimal
378 theoretical stress orientation (bounded by the 90% confidence interval) corresponding to
379 the slip on each fault. We applied the Wallace-Bott hypothesis that predicts the motion
380 on a (fault) surface to be parallel to the direction of the greatest resolved shear stress.
381 The underlying assumptions of this hypothesis are planar (fault) surfaces, rigid hosting
382 rock, uniform stress state and absence of stress perturbations or rotations along the
383 plane. Following Yamaji (2007), we assumed that this hypothesis is valid for newly
384 forming and reactivated fault planes. Thus the shear τ and the normal vector σ_N

385 components of a stress tensor T acting on a fault plane are (e.g., Angelier, 1994; Xu,
386 2004; Alberti 2010):

$$\tau = \sigma - \sigma_N \quad (6)$$

$$\sigma_N = n^t(n\sigma) \quad (7)$$

387 where σ is the stress vector, n is the normal unit vector and n^t is the transpose.

388 Although the Wallace-Bott hypothesis is a simplification of the underlying rock
389 mechanics, its validity has been shown by field observations and empirical
390 demonstrations (e.g., Zoback et al., 1981; Le Pichon et al., 1988) as well as by
391 numerical models and comparisons with different methods (Dupin et al., 1993; Pollard
392 et al., 1993; Pascal, 2002).

393 Applying this approach, the maximum shear stress direction is assumed to be the likely
394 sense of motion between the fault blocks and can be compared to the fault's rake.
395 Because the shear stresses on faults depend on the orientations of the stress field axes
396 with respect to the fault's orientation and on the stress ratio $R = (S_2 - S_3)/(S_1 - S_3)$,
397 the stress tensor has a theoretical maximum shear stress direction on any fault plane.
398 However, the Coulomb-Navier criterion states that a failure fracture occurs on the
399 (fault) plane where the critical shear stress reaches the cohesive strength (σ_0) of the
400 hosting rock plus an increment of shear equal to the product of the normal stress (σ_N)
401 acting on the plane and the hosting rock friction coefficient (μ). This criterion is
402 graphically represented in stress space by Mohr's circle and two lines intersecting the
403 shear axis at $\pm \sigma_0$ with the slope $\pm \mu$. The intersection of the Mohr's stress circle and the
404 straight line of the Coulomb-Navier criterion occurs at an angle 2θ , where θ represents
405 the angle between σ_1 and the fault plane (Ranalli, 1987). The Coulomb-Navier criterion
406 gives a satisfactory account of shear fracture both in the laboratory and the field
407 (Ranalli, 1987) and empirically shows that:

$$\tan 2\theta = 1/\mu \quad (8)$$

408 Applying Eq. 8 to all possible ranges of fault friction (e.g., between 0 and 1), the
409 corresponding angle between S1 and the fault plane corresponds to $22.5^\circ \leq \theta \leq 45^\circ$.

410

411 The determination of the stress tensors compatible with parameters of each active fault
412 was carried out in a three-step procedure. We first generated S1, S2 and S3 trends and
413 plunge values at regular intervals to explore a wide range of possible stress tensors
414 orientations. In the next step, we considered only the stress tensors satisfying the
415 $22.5^\circ \leq \theta \leq 45^\circ$ conditions and S3 positioned in the compression quadrant. The
416 resulting stress tensors were then used as input values in the ForwardStress code
417 (Alberti, 2010) to calculate the maximum resolved shear stress for each interpolation
418 point along the studied faults. We calculated the SHmax orientation using the "alpha"
419 function of Lund and Townend (2007) for those faults with a rake interval (as defined in
420 the EDSF database) corresponding to the maximum resolved shear stress. To calculate
421 the SHmax *posterior* uncertainties based on the assumed uniform probability
422 distribution of the strike and dip min-max intervals, we repeated the stress tensor
423 selection at regular steps for both the strike and dip values. In the last step, we
424 determined the final SHmax orientation as the central value of the most populated 1°-
425 wide bin in the 0°-180° range. Accordingly, the 90% bounds of the generated SHmax
426 orientations, defined as the 90% confidence level of the theoretical SHmax, represent
427 the condition under which the faults are considered to be positively oriented.

428 In the following text, we refer to SHmax orientations obtained by this method as the
429 theoretical SHmax.

430

431 On the same 258 nodes along the fault's upper edges, we interpolated the SHmax data
432 records with SHINE using WSM08 (Heidbach et al, 2008). Therefore, in the data
433 selection part of SHINE, we chose the WMS08 dataset, while in the "Geographic
434 setting" we chose the "Custom input file" option. We defined the "Searching radius" as
435 three (data records within a 96 km radius), the "Minimum cluster" as three and the 90%
436 confidence bounds as 40° . We kept the confidence level reasonably low to ensure stable
437 results. Application of these parameters resulted in 257 SHmax orientations (Figure 7),
438 we note that only one point did not satisfy the chosen SHINE input parameters (its 90%
439 confidence bound reached 47° and was therefore excluded from further consideration).
440 In the following text we refer to SHmax orientations obtained by this method as SHINE
441 SHmax.

442

443 To compare SHINE and theoretical SHmax orientations, we calculated the angular
444 difference β between both median values at each interpolation point. The value of β is
445 therefore a measure of the compatibility between the SHINE and theoretical SHmax
446 orientation. For each interpolation, we ranked the compatibility between both SHmax
447 orientations in five classes; A ($0^\circ \leq \beta \leq 15^\circ$), B ($15^\circ < \beta \leq 25^\circ$), C ($25^\circ < \beta \leq 35^\circ$),
448 D ($35^\circ < \beta \leq 45^\circ$), E ($\beta > 45^\circ$). The A-C classes imply a kinematically correlated
449 fault slip sense in the present-day stress regime. We consider faults with D class results
450 still being able to be active in a given stress regime, while we set E class faults to have
451 uncorrelated theoretical slip direction in the present-day stress regime.

452 The class-type breakdown of the the 257 analyzed nodes shows 104 to belong to class
453 A, 52 to B and C classes, 37 to D and 12 to E (Figure 8). The E- ranked interpolation
454 points belong to four active faults. Half of them belong to ATCS011, a fault that also
455 has the maximum 72° β misfit. The other three faults with E class nodes lie on faults in
456 the northern and central part of the study area. The spatial distribution of hosting D

457 class fault nodes shows a similar pattern, with the majority of them located in the
458 northern and central parts, and some belonging to ITCS101, SICS006, SICS010 and
459 HRCS037 faults. A majority of faults hosting A- and B- ranked interpolation points lie
460 in the southern part of the study area, with exception of few faults in the centre and
461 north (for example SICS007, SICS008, SICS012, SICS023).

462

463 The ATCS011 is an active fault with considerable length. The fault length appears to
464 have an influence on the SHmax orientation discordance given the fault's minimum-
465 maximum strike interval is between 260° and 300° over distances larger than 100 km,
466 while its rake varies between 130° - 170° . Such conditions do not capture the local
467 conditions well because they generalize characteristics over long distances. Along the
468 ATCS011 down-dip projection, a focal mechanism of the 2nd February, 2013 M_w 4.05
469 gives a P-axis azimuth of 199°
470 (http://www.eas.slu.edu/eqc/eqc_mt/MECH.EU/20130202133535/index.html) which is
471 in better agreement with the SHINE than the theoretical SHmax orientation. Overall,
472 this approach provides a practical example of applying SHINE to test the relationship
473 between an observed set of faults and the in-situ stress field.

474

475 The ITCS101 fault has D class misfit nodes in its north-western section. The location of
476 this fault corresponds to the intersection of the NW-SE oriented dextral strike-slip faults
477 of the External Dinarides and the E-W oriented thrust of the Southern Alps. In this case
478 a more detailed revision of the available geological, seismic and seismological data
479 might offer a better understanding of the geometry and kinematics of active faults.

480

481 The faults in central Slovenia host both the highest and lowest β value points. These
482 differences are due to the low density and scattered orientations of the input data-
483 records for the area. The focal mechanism solutions (Ložar Stopar and Živčić, 2007;
484 Ložar Stopar and Živčić, 2008) confirm the ESFD geometric and kinematic fault
485 parameters, whereas SHINE SHmax orientation suggests thrust kinematics for some of
486 those faults (SICS013).

487 Using SHINE it is possible to evaluate the degree of kinematic compatibility between
488 active faults and the in-situ stress field. In the case of strong incompatibility, we
489 recommend that the contributing researchers further investigate this discrepancy, paying
490 attention to the original fault data. Similarly, we suggest double checking the original
491 stress data records that were used for the determining SHmax orientation. As shown by
492 Carafa and Barba (2013), the spatial distribution and density coverage of input stress
493 data records significantly influences the reliability of the SHmax orientation. Such
494 considerations might be important when planning and funding future fault data analyses
495 and SHmax measurements.

496

497 **6. Conclusions**

498 The dissemination and sharing of knowledge is facilitated by an effective and coherent
499 plan for the development of software tools intended for use by the community. With this
500 work, we described all steps we performed to create an effective web service
501 (<http://shine.rm.ingv.it/>). The primary goal of the SHINE software is to provide an
502 efficient stress interpolation technique - this goal was optimized by focusing on the end
503 user perspective. For any geoscientist, SHINE sets a base level for determining SHmax
504 orientations because it incorporates robust analytical formulations into stress map
505 creation, thereby offering discrete quantitative results, not just a visual comparison of

506 SHmax orientations distributions on a map. Moreover, the logfile that is included in the
507 final downloadable zipped file registers all of the selected input parameters of each
508 interpolation, which satisfies the reproducibility principle for any calculated SHmax
509 map.

510

511 A SHINE application for a comparison between the theoretical and observed fault
512 SHmax orientations was provided as an illustrative example of its utility and
513 applicability for active tectonics research. In this case, SHINE was used as a tool to test
514 fault compatibility in the present-day stress regime. This is just one of the potential
515 applications, which is useful for researchers working in different disciplines ranging
516 from geodynamics to field geology. SHINE's underlying rationale can be summed up by
517 three words: usability, effectiveness and efficiency. These principles will be the road
518 map for future SHINE development and integrations.

519

520 ***Acknowledgments***

521 This work was entirely funded by the project MIUR-FIRB 'Abruzzo' (code:
522 RBAP10ZC8K_003). We thank the SHINE website test-user researchers for their
523 opinions. We acknowledge the suggestions from the Editor Jef Caers and an anonymous
524 reviewer for useful remarks. We also thank D. Sorrentino and A. De Santis for their
525 work on maintaining SHINE's hosting server.

526

527 **References**

- 528 Alberti, M. (2010), Analysis of kinematic correlations in faults and focal mechanisms
529 with GIS and Fortran programs, *Comput. Geosci.*, *36*(2), 186–194,
530 doi:10.1016/j.cageo.2009.06.006.
- 531 Angelier, J. (1994), Paleostress analysis of small-scale brittle structures., in *Continental*
532 *Deformation*, edited by P. Hancock, pp. 53– 100, Pergamon.
- 533 Basili, R. et al. (2013), The European Database of Seismogenic Faults (EDSF) compiled
534 in the framework of the Project SHARE, , doi:10.6092/INGV.IT-SHARE-EDSF.
535 Available from: <http://diss.rm.ingv.it/share-edsf/>
- 536 Bird, P., and Y. Li (1996), Interpolation of principal stress directions by nonparametric
537 statistics: Global maps with confidence limits, *J. Geophys. Res.*, *101*, 5435–5443.
- 538 BSI (1998), ISO 9241-11:1998, Ergonomic requirements for office work with visual
539 display terminals (VDTs) - Part 11: Guidance on usability,
- 540 Carafa, M. M. C., and S. Barba (2013), The stress field in Europe: optimal orientations
541 with confidence limits, *Geophys. J. Int.*, *193*(2), 531–548, doi:10.1093/gji/ggt024.
- 542 Coblenz, D., and R.M. Richardson, Statistical Trends in the Intraplate Stress Field,
543 *Journal of Geophysical Research*, *100*, 20,245-20,255, 1995.
- 544 Dupin, J.-M., W. Sassi, and J. Angelier (1993), Homogeneous stress hypothesis and
545 actual fault slip: a distinct element analysis, *J. Struct. Geol.*, *15*(8), 1033–1043,
546 doi:10.1016/0191-8141(93)90175-A.
- 547 Heidbach, O., M. Tingay, A. Barth, J. Reinecker, D. Kurfeß, and B. Müller (2008), The
548 World Stress Map database release 2008, , doi:10.1594/GFZ.WSM.Rel2008.

- 549 Kastelic, V., and M. M. C. Carafa (2012), Fault slip rates for the active External
550 Dinarides thrust-and-fold belt, *Tectonics*, 31, TC3019,
551 doi:10.1029/2011TC003022.
- 552 Kastelic, V., M. Vrabc, D. Cunningham, and A. Gosar (2008), Neo-Alpine structural
553 evolution and present-day tectonic activity of the eastern Southern Alps: The case
554 of the Ravne Fault, NW Slovenia, *J. Struct. Geol.*, 30(8), 963–975,
555 doi:10.1016/j.jsg.2008.03.009.
- 556 Le Pichon, X., F. Bergerat, and M.-J. Roulet (1988), Plate kinematics and tectonics
557 leading to the Alpine belt formation: A new analysis, in *Processes in Continental*
558 *Lithospheric Deformation*, edited by S. P. Clark, J. B. C. Burchfiel, and J. Suppe,
559 pp. 111–131.
- 560 Lee, J.-C., and J. Angelier (1994), Paleostress trajectory maps based on the results of
561 local determinations: the “lissage” program, *Comput. Geosci.*, 20(2), 161–191,
562 doi:10.1016/0098-3004(94)90004-3.
- 563 Ložar Stopar, M., and M. Živčić (2007), Fault plane solutions of some stronger
564 earthquakes in Slovenia in 2005, in *Earthquakes in 2005*, edited by Environmental
565 Agency of the Republic of Slovenia Seismology and Geology Office, pp. 57–62.
- 566 Ložar Stopar, M., and M. Živčić (2008), Fault plane solutions of some stronger
567 earthquakes in Slovenia in 2006 and 2007, in *Earthquakes in 2007*, edited by
568 Environmental Agency of the Republic of Slovenia Seismology and Geology
569 Office, pp. 48–53.
- 570 Lund, B., and J. Townend (2007), Calculating horizontal stress orientations with full or
571 partial knowledge of the tectonic stress tensor, *Geophys. J. Int.*, 1328–1335,
572 doi:10.1111/j.1365-246X.2007.03468.x.

- 573 Müller, B., V. Wehrle, S. Hettel, B. Sperner, and K. Fuchs (2003), A new method for
574 smoothing orientated data and its application to stress data, *Geol. Soc. London,*
575 *Spec. Publ.*, 209(1), 107–126, doi:10.1144/GSL.SP.2003.209.01.11.
- 576 Nah, F. (2004), A Study on Tolerable Waiting Time: How Long Are Web Users Willing
577 to Wait?, *Behav. Inf. Technol.*, 23(3), 153–163.
- 578 Nielsen, J. (2000), *Web usability*, Apogeo Editore.
- 579 Pascal, C. (2002), Interaction of faults and perturbation of slip: influence of anisotropic
580 stress states in the presence of fault friction and comparison between Wallace–Bott
581 and 3D Distinct Element models, *Tectonophysics*, 356(4), 307–322,
582 doi:10.1016/S0040-1951(02)00413-4.
- 583 Placer, L. (1998), Contribution to the macrotectonic subdivision of the border region
584 between southern Alps and External Dinarides, *Geologija*, 41, 223–255.
- 585 Poljak, M. (2000), Structural-Tectonical Map of Slovenia 1 : 250.000, *Geol. Surv.*
586 *Slov.*
- 587 Pollard, D. D., S. D. Saltzer, and A. M. Rubin (1993), Stress inversion methods: are
588 they based on faulty assumptions?, *J. Struct. Geol.*, 15(8), 1045–1054,
589 doi:10.1016/0191-8141(93)90176-B.
- 590 Ranalli, G. (1995), *Rheology of the Earth*, Springer.
- 591 Sperner, B., B. Müller, O. Heidbach, D. Delvaux, J. Reinecker, and K. Fuchs (2003),
592 Tectonic stress in the Earth's crust: advances in the World Stress Map project, The
593 Geological Society, London.

- 594 Stone, D., C. Jarrett, M. Woodroffe, and S. Minocha (2005), *User interface design and*
595 *evaluation*, Elsevier : Morgan Kaufmann, Amsterdam.
- 596 Stucchi, M. et al. (2013), The SHARE European Earthquake Catalogue (SHEEC) 1000–
597 1899, *J. Seismol.*, 17(2), 523–544, doi:10.1007/s10950-012-9335-2.
- 598 Vrabc, M., and L. Fodor (2006), Late Cenozoic Tectonics Of Slovenia: Structural
599 Styles At The Northeastern Corner Of The Adriatic Microplate, edited by N.
600 Pinter, G. Gyula, J. Weber, S. Stein, and D. Medak, pp. 151–168, Springer
601 Netherlands.
- 602 Wroblewski, L. (2008), *WEB FORM DESIGN Filling in the Blanks*.
- 603 Xu, P. (2004), Determination of regional stress tensors from fault-slip data, *Geophys. J.*
604 *Int.*, 157(3), 1316–1330, doi:10.1111/j.1365-246X.2004.02271.x.
- 605 Yamaji, A. (2007), *An Introduction to Tectonophysics: Theoretical Aspects of*
606 *Structural Geology*, Terrapub.
- 607 Živčić, M. (2010), Earthquake catalogue, unpublished material, *Off. Seismol. Geol.*
608 *Agency Repub. Slov. Environ.*
- 609 Zoback, M. D., and M. L. Zoback (1981), State of stress and intra-plate earthquakes in
610 the central and eastern United States, *Science*, 213, 96–104.
- 611 Zoback, M. Lou, and M. D. Zoback (1989), Tectonic stress field of the continental
612 United States, *Geol. Soc. Am. Mem.*, 172, 523–540, doi:10.1130/MEM172-p523.
- 613

614 **Figure Captions**

615 Figure 1. System architecture described in this paper.

616

617 Figure 2. A view of the SHINE start page.

618

619 Figure 3. A view of the Data Selection section.

620

621 Figure 4. A view of the Geographical Setting section.

622

623 Figure 5. A view of the Strategic Parameters section.

624

625 Figure 6. A view of the Results visualization. At the bottom of the Results page, in blue,

626 there is the link for downloading the results (provided in several GIS formats) as a zip

627 file.

628

629 Figure 7. SHmax orientation (thin blue lines) resulting from SHINE interpolating the

630 WSM08 data, (thick red lines). Fault upper edge traces, shown as name-labeled orange

631 lines, taken from EDSF (Basili et al., 2013).

632

633 Figure 8. Angular difference (β) between the theoretical SHmax and SHINE SHmax for

634 interpolation points of the studied active faults. Different β classes are color-coded as

635 shown in the legend.

636

637 **HIGHLIGHTS**

638 - SHINE incorporates an innovative interpolation technique and a user-friendly GUI;

639 - SHINE quickly visualizes results, downloadable in several formats;

640 - SHINE rationale is summed up by 3 words: usability, effectiveness and efficiency.

641

Figure 1

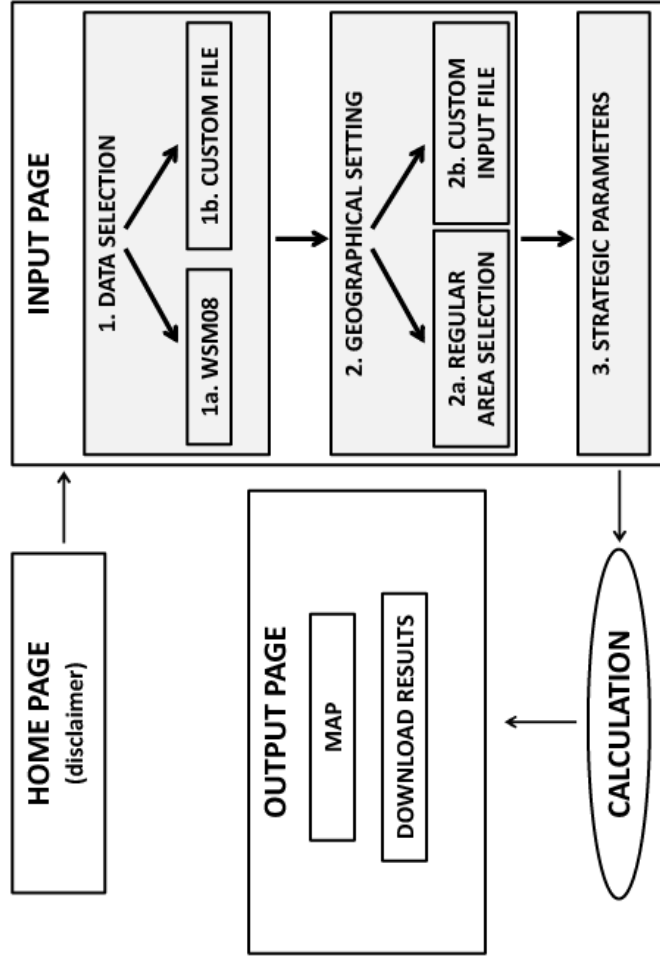


Figure 2

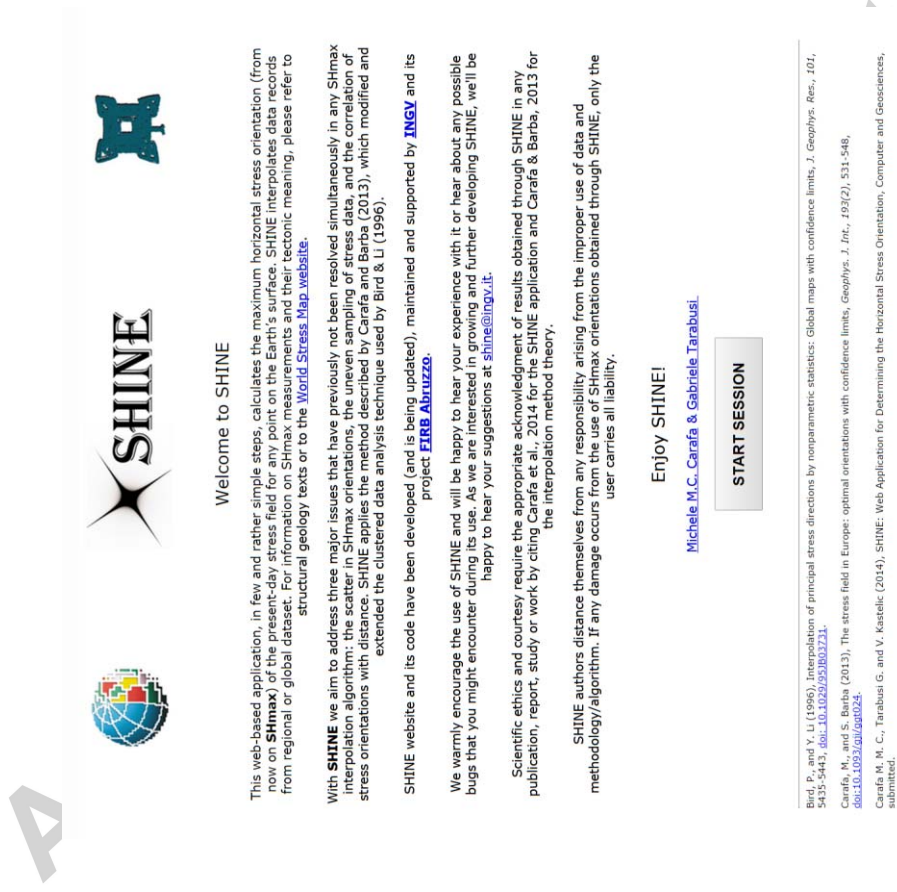


Figure 3

A



Figure 4

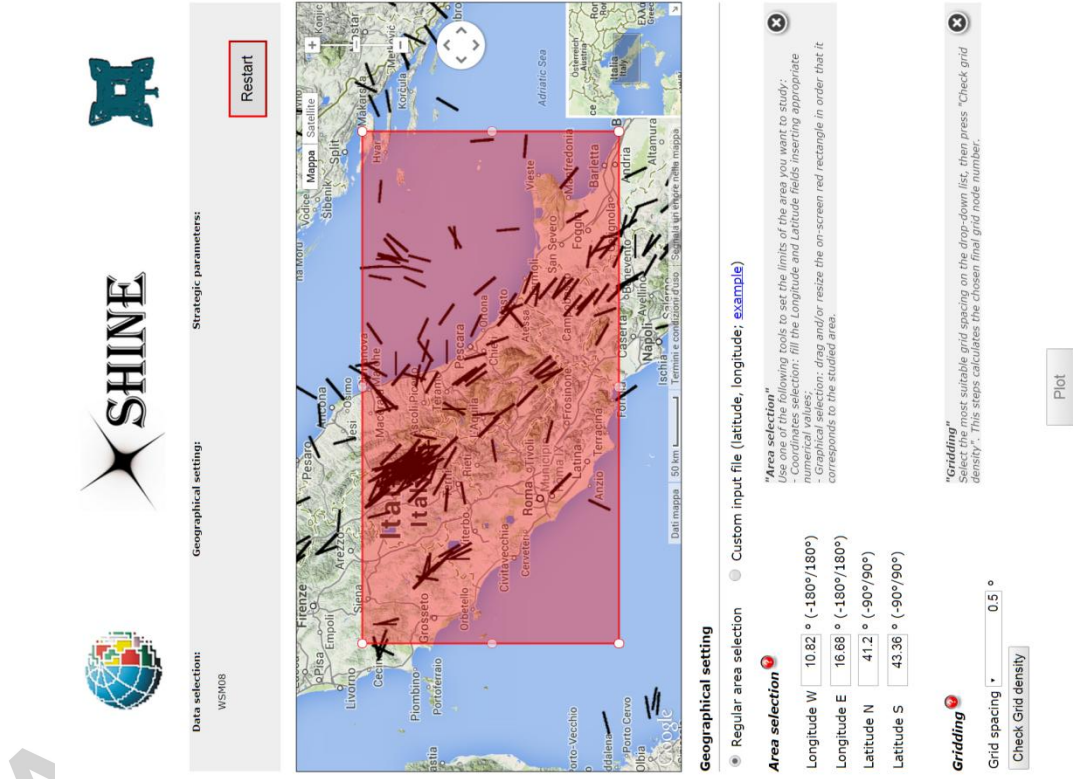


Figure 5

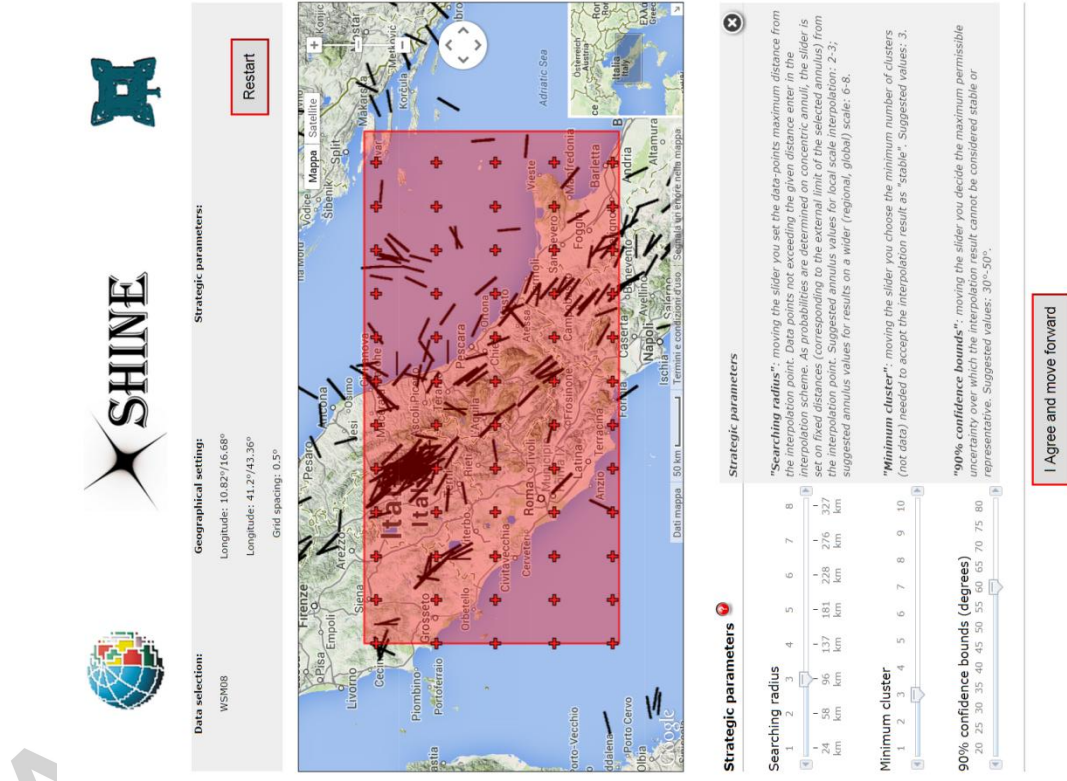


Figure 6

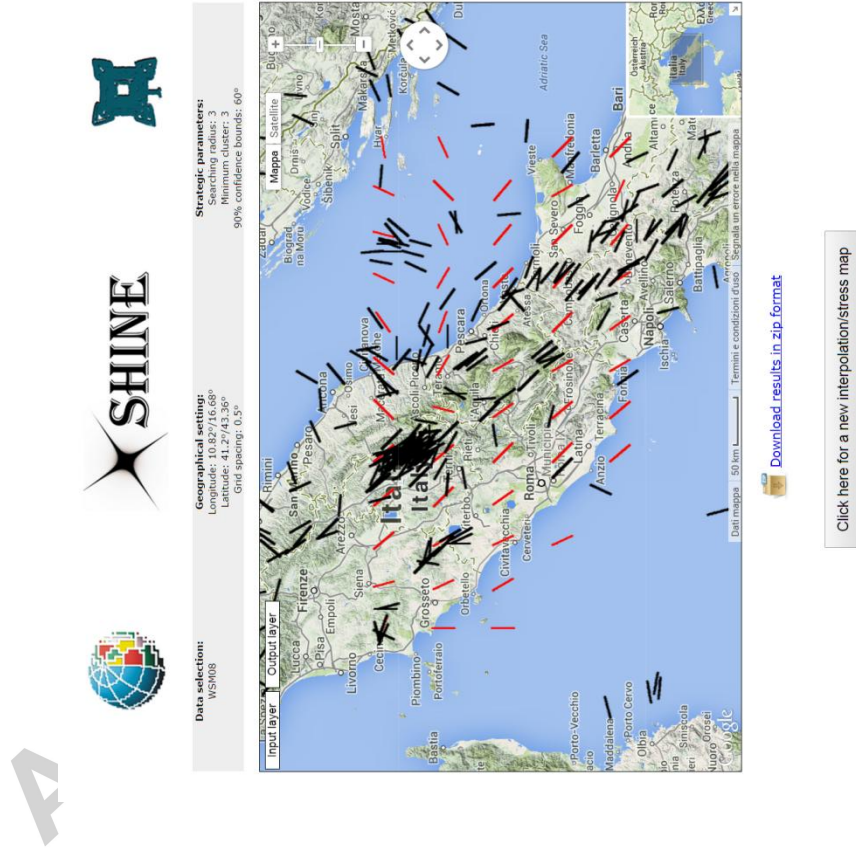


Figure 7

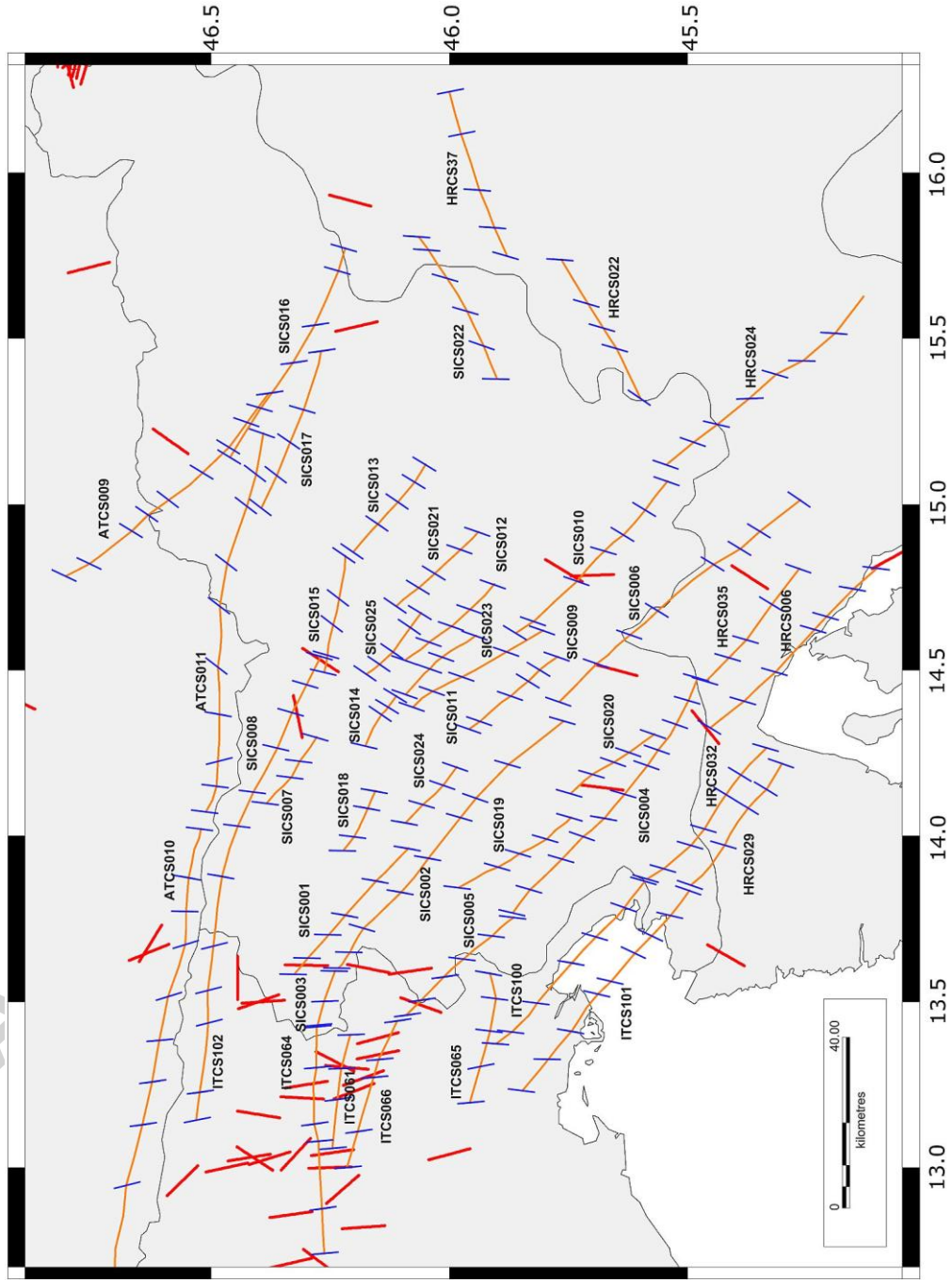
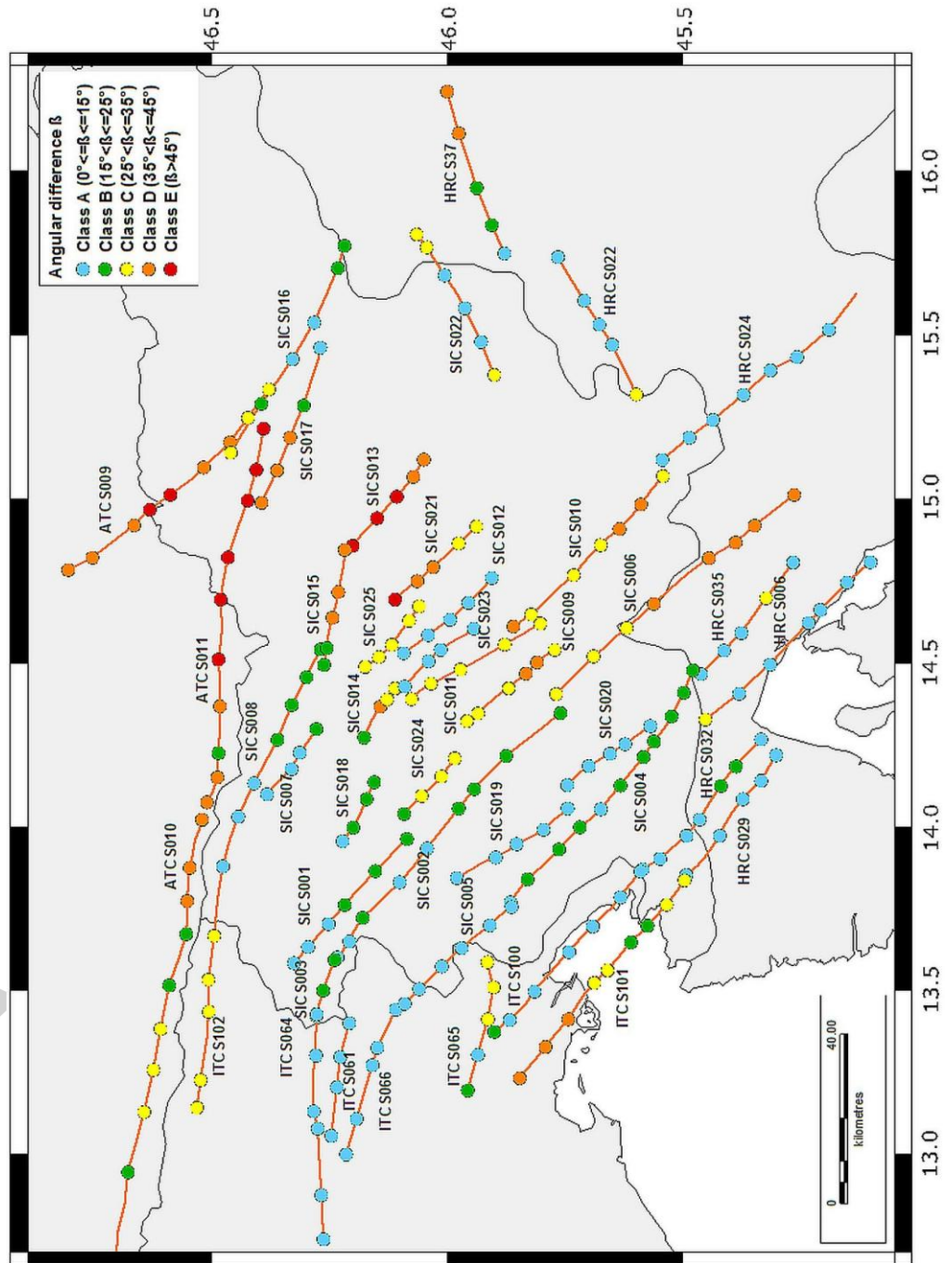


Figure 8





Horizontal Most Compressive Stress
Axis Interpolation

Welcome to SHINE



Progetto ABRUZZO

This web-based application, in few and rather simple steps, calculates the maximum horizontal stress orientation (from now on SHmax) of the present-day stress field for any point on the Earth's surface. SHINE interpolates data records from regional or global dataset. For information on SHmax measurements and their tectonic meaning, please refer to structural geology texts or to the [World Stress Map website](http://www.world-stress-map.org).

With SHINE we aim to address three major issues that have previously not been resolved simultaneously in any SHmax interpolation algorithm: the scatter in SHmax orientations, the uneven sampling of stress data, and the correlation of stress orientations with distance. SHINE applies the method described by Carafa and Barba (2013), which modified and extended the clustered data analysis technique used by Bird & Li (1996).

SHINE website and its code have been developed (and is being updated), maintained and supported by INGV and its project [EIRB ABRUZZO](http://www.eirb-abruzzo.it).

We warmly encourage the use of SHINE and will be happy to hear your experience with it or hear about any possible bugs that you might encounter during its use. As we are interested in growing and further developing SHINE, we'll be happy to hear your suggestions at shine@ingv.it.

Scientific ethics and courtesy require the appropriate acknowledgment of result publication, report, study or work by citing Carafa et al., 2014 for the SHINE app and the interpolation method theory.

SHINE authors distance themselves from any responsibility arising from the methodology/algorithm. If any damage occurs from the use of SHmax orientation user carries all liability.

Enjoy SHINE!

[Michele M.C. Carafa & Gabriele Tarabusi](#)

START SESSION

Bird, P., and V. Li (1996). Interpolation of principal stress directions by nonparametric statistics: Global map 5435-5443, doi:10.1029/1995JB02331.

Carafa, M., and S. Barba (2013). The stress field in Europe: optimal orientations with confidence limits, *Geophysical Research Letters*, doi:10.1029/2012GL052028.

Carafa M., M. C. Tarabusi G. and V. Kastelic (2014), SHINE: Web Application for Determining the Horizontal stress field, submitted.

<http://shine.rm.ingv.it/>

